RESEARCH ARTICLE | FEBRUARY 10 2026

Correlation of coercivity, microstructure, and surface defects in HDDR-processed Nd-Fe-B powders for bonded magnet applications

X. B. Liu ; M. S. Kesler ; Z. P. Tener ; M. J. Kramer ; M. A. McGuire ; I. C. Nlebedim

AIP Advances 16, 025022 (2026)
https://doi.org/10.1063/9.0001013
CHORUS

Correlation of coercivity, microstructure, and surface defects in HDDR-processed Nd-Fe-B powders for bonded magnet applications

Cite as: AIP Advances 16, 025022 (2026); doi: 10.1063/9.0001013
Submitted: 6 October 2025 • Accepted: 7 December 2025 •
Published Online: 10 February 2026

X. B. Liu,[1,a] M. S. Kesler,[2] Z. P. Tener,[2] M. J. Kramer,[1,3] M. A. McGuire,[2] and I. C. Nlebedim[1,b]

AFFILIATIONS

[1] Critical Materials Innovation Hub, Division of Critical Materials, Ames National Laboratory, US DOE, Ames, Iowa 50011, USA
[2] Materials Science and Technology Division, Oak Ridge National Laboratory, Oak Ridge, Tennessee 37831, USA
[3] Department of Materials Science and Engineering, Iowa State University, Ames, Iowa 50011, USA

Note: This paper was presented at the 70th Annual Conference on Magnetism and Magnetic Materials.
[a] **Author to whom correspondence should be addressed:** liux@ameslab.gov
[b] **Email:** nlebedim@ameslab.gov

ABSTRACT

Hydrogenation-Disproportionation-Desorption-Recombination (HDDR) is an effective method for producing high coercivity, anisotropic powder from either fresh Nd-Fe-B alloy or recycled Nd-Fe-B magnets for use in bonded magnets. We investigated the impact of surface defects on the coercivity of HDDR-processed Nd-Fe-B using scanning electron microscopy (SEM), magnetic measurements, and micromagnetic simulations. We observed that coercivity decreases as particle size reduces, with SEM revealing surface defects and the detachment of $Nd_2Fe_{14}B$ grains and Nd-rich phases from the particle surface. Micromagnetic simulations indicate that demagnetization initiates at the particle surface, where these defects are most concentrated, leading to reduced coercivity. The reduction in squareness of demagnetization curve, knee point field and coercivity for smaller HDDR particles is attributed to an increased specific surface area, which exhibits reduced nucleation field and weak domain wall pinning field during magnetization reversal. By addressing the role of surface defects in coercivity degradation, this study provides insights for improving both new powder production and recycling strategies, ultimately leading to enhanced performance of bonded magnets and contributing to more sustainable practices in the rare earth supply chain. One potential strategy to enhance the performance of HDDR Nd-Fe-B materials involves reducing the fraction of fine particles (<35 μm) and promoting the formation of grain boundary phases on particle surfaces.

I. INTRODUCTION

High-performance Nd-Fe-B magnets have been widely applied in electric vehicles and consumer electronics.[1–3] The hydrogenation-disproportionation-desorption-recombination (HDDR) process is an effective method to produce high coercivity anisotropic powder for bonded magnets[4–10] and has recently been extended to remanufacture the end-of-life (EOL) Nd-Fe-B into anisotropic magnetic powder.[11–13] Under optimized HDDR processing conditions, the resulting Nd-Fe-B powder has a typical $Nd_2Fe_{14}B$ grain size of ~300-500 nm and a strong *c*-axis crystal texture, which enables high coercivity and strong magnetic anisotropy.[4,14–17] Nonetheless, typical coercivity values of HDDR ternary Nd-Fe-B (~9-13 kOe) are comparable to those of sintered ternary Nd-Fe-B magnets (12-15 kOe), with a grain size of 3-8 μm, which limits some applications. A deeper understanding of the demagnetization mechanism in HDDR Nd-Fe-B is therefore crucial for developing an effective approach to improve coercivity.

In addition to the intrinsic magnetic properties such as magnetocrystalline anisotropy (MCA), the coercivity is also sensitive to microstructure in Nd-Fe-B magnet. The most critical factors are grain size and Nd-rich grain boundary phase (GBP). The coercivity increases almost logarithmically with decreasing average grain size in Nd-Fe-B sintered magnets, as expressed $H_{ci} = a - b \ln D$ according

to Ramesh *et al.*[18] The *a* and *b* are fitted parameters, and *D* is the average grain size. Following this empirical formula, the Nd-Fe-B magnet with an average grain size of 300-600 nm should have a coercivity larger than 22 kOe.[19] The relatively low coercivity (9–13 kOe) observed in fine-grained HDDR Nd-Fe-B powder suggests that other microstructural features play a more significant role in determining its coercivity.

In this work, we have studied the effect of microstructure and surface defects on coercivity in HDDR Nd-Fe-B using scanning electron microscopy (SEM), magnetic measurements, and micromagnetic simulations. The correlation between surface defects and coercivity has been discussed. Finally, we discuss the potential approach to mitigate the negative effect of surface defects and enhance coercivity.

II. EXPERIMENTAL AND COMPUTATIONAL DETAILS

Arc-melted $Nd_{14}Fe_{77.9}B_7AlCu_{0.1}$ alloys were mechanically crushed into coarse-size powder (1-3mm) and subsequently used as feedstock for HDDR process. The feedstock was heat-treated at 800 °C for 90 min under a H_2 pressure of 400 kPa, followed by a treatment at 820 °C for 15 min under a H_2 pressure of 5 kPa, and then a vacuum (less than 0.1 Pa) heat treatment at 800 °C for 30 min. The details of the sample preparation have been previously reported.[17] The microstructure was observed in a Field-Emission Scanning Electron Microscope (FE-SEM, FEI Teneo). To evaluate the effect of particle size on the magnetic properties, the HDDR-processed Nd-Fe-B powder is classified using sieving. The powder was mixed with paraffin wax and cooled from 323 K to 300 K while being aligned under a magnetic field of 30 kOe. Magnetic hysteresis loops of the samples were obtained using a Quantum Design SQUID MPMS-3 vibrating sample magnetometer (VSM) with an applied magnetic field up to 70 kOe. No demagnetization factor correction is performed for the measured magnetic hysteresis loop. The squareness(Q) of the demagnetization curve was estimated by the ratio of the knee point field (H_k) over the intrinsic coercivity (H_{ci}), i.e., $Q = H_k/H_{ci}$. H_k is the external field at 90% of remanence J_r on the *J-H* demagnetization curve.[20]

Micromagnetic simulation has been an effective method at the continuum level to model the static and dynamic magnetic properties, which is based on Landau-Lifshitz-Gilbert equation (LLG).[21–23] We perform micromagnetic modeling using a finite difference (FD) micromagnetic code MuMax3.[24,25] We adopt a finite-difference cell size of 1 × 1 × 1 nm for all the calculations. A field step of 2 mT is used to calculate the magnetic hysteresis loop. The total energy minimization was performed using a conjugate gradient method with a convergence criterion of a normalized magnetization change of less than 10^{-6}. Additional details of the micromagnetic simulation were also previously reported.[26] The material parameters of $Nd_2Fe_{14}B$ in the micromagnetic simulation are taken from literature.[27] Magnetization J_s, magnetocrystalline anisotropy constant K_1, and exchange constant A are 1.6 T, 4.5 MJ/m^3 and 9 pJ/m, respectively.

III. RESULTS AND DISCUSSION

A. Magnetic properties of HDDR-processed Nd-Fe-B powder

To evaluate the effect of particle size on magnetic properties, the as-prepared HDDR Nd-Fe-B powder was classified into different sizes using sieving, and the *J-H* magnetic hysteresis loops measurements for each size are displayed in Fig. 1(a). As expected, the magnetization J_s (~14 kG under a field of 70 kOe) remains almost unchanged. However, the coercivity (H_{ci}), knee point field (H_k), and squareness (Q) of the *J-H* demagnetization curves decreased with decreasing particle size (Fig. 1(b)). For the 106 – 125 μm particles, the values of H_{ci}, H_k, and Q are 14.0 kOe, 5.5 kOe, and 0.387, respectively. However, the < 32 μm powder has an H_{ci} of 12.2 kOe, an H_k of 2 kOe, and a Q of 0.16. These decreasing trends indicate the existence of more regions with weak nucleation or domain wall de-pinning sites in those HDDR Nd-Fe-B particles during the magnetization reversal process.

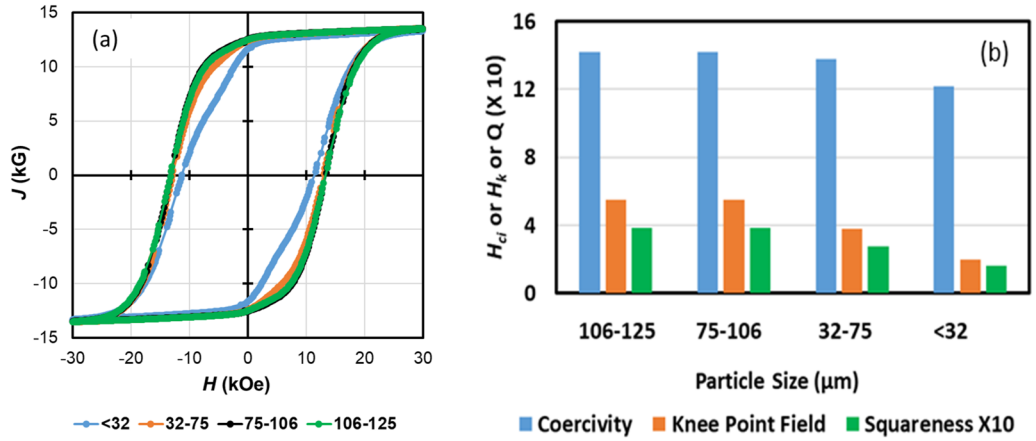

FIG. 1. Magnetic hysteresis loop *J-H* for HDDR-processed Nd-Fe-B powder with different particle sizes (a) and their particle size dependence of coercivity H_{ci} (kOe), knee point field H_k (kOe) and squareness, Q. The labels <32, 32–75, 75–106, and 106–125 correspond to particle size ranges of less than 32 μm, 32–75 μm, 75–106 μm, and 106–125 μm, respectively. For visualization purposes, the value of Q shown is scaled by a factor of 10.

As we will discuss in Sec. III B, surface defects exist in HDDR-processed Nd-Fe-B powder, which deteriorate coercivity of the surface layer. As particle size decreases, the specific surface area increases. Assuming all particles have the same shape and a uniform surface layer thickness, the volume fraction of the surface defect layer will increase rapidly with decreasing particle size. The low coercivity of the surface layer contributes to the deteriorated squareness of the demagnetization curve, lower knee field and coercivity for fine particles (Fig. 1(b)).

B. Microstructure of HDDR-processed Nd-Fe-B powder

The particle surface is expected to have more structural defects due to atomic reconstruction and/or oxidation, resulting in Nd deficiency and weak local MCA. These defects also deteriorate the formation of Nd-rich GBP. To clarify the role of the surface defect, we investigated the microstructure on the surface and inside the HDDR Nd-Fe-B powder.

As shown in Fig. 2(a), the HDDR powder exhibits an irregular shape and a large size distribution, ranging from several tens to several hundred microns. Figures 2(b) and 2(c) show the microstructure on the particle surface and inside the particle, respectively. The enlarged surface microstructure is displayed in Fig. 2(d) to reveal further structural details. The typical grain size of 2:14:1 ranges from 200–600 nm on the particle surface and inside the particle (Figs. 2(b)–2(d)). As observed by SEM, there is a lack of Nd-rich GBP on the particle surface, which would reduce coercivity (Fig. 2(d)). One possible reason is that the Nd-rich phase on the particle surface would readily oxidize. Also, we observed detached, isolated $Nd_2Fe_{14}B$ grains on the particle surface. The particle surface roughness is about 2-3 times the $Nd_2Fe_{14}B$ (2:14:1) average grain size (Fig. 2(b)). Those defects can reduce the critical domain nucleation and domain wall pinning fields of the surface layer during magnetization reversal, which are confirmed by our micromagnetic simulation in Sec. III C.

Figure 2(c) shows an SEM image of the polished sample of HDDR Nd-Fe-B powder, revealing the microstructure inside the particle. The typical grain size of primary phase 2:14:1 is the same as that on the particle surface (200-600 nm), as observed on the particle surface. In contrast to the surface microstructure, the Nd-rich GBP does exist and surrounds the grains of the primary phase 2:14:1 (Fig. 2(c), white phase). The GBP can effectively pin domain walls and prevent them from moving into neighboring 2:141 grains during the magnetization reversal process, which enhances the coercivity.

C. Micromagnetic simulation

To gain a deep understanding of the effect of surface microstructure on the hard magnetic properties in HDDR-processed Nd-Fe-B particles. We perform micromagnetic simulations for several Nd-Fe-B magnetic particles with different microstructure features. Figure 3 shows the spatially resolved magnetization distribution of a cube-shaped Nd-Fe-B particle with an edge length of 128 nm under different external fields. It has an average grain size of 40 nm and the *c*-axis of 2:14:1 grain aligned along the *z*-axis direction. It reveals that magnetization reversal

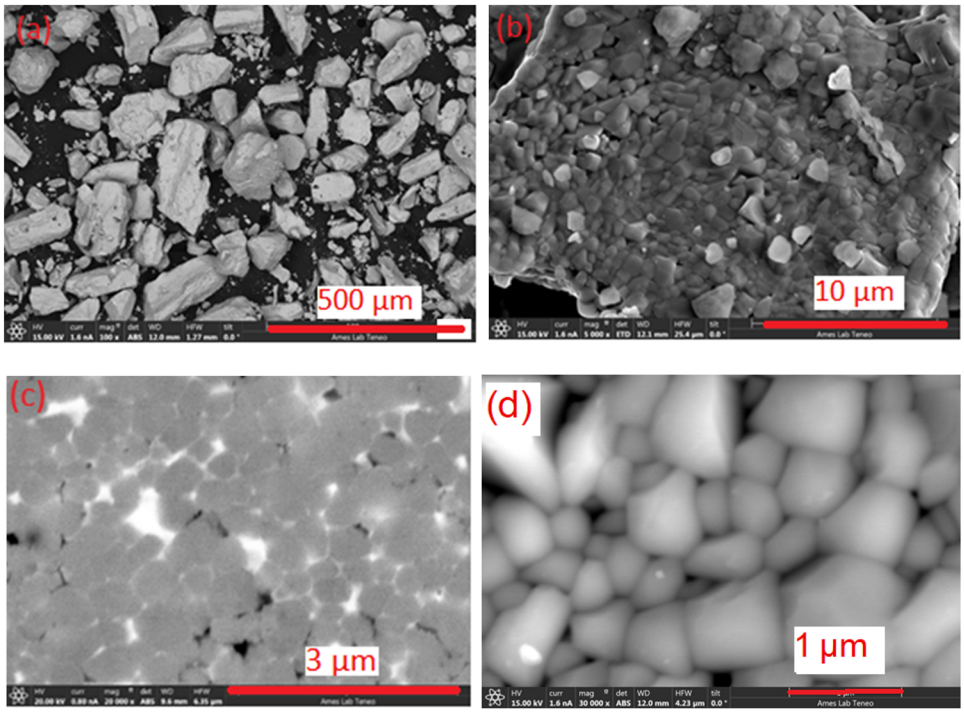

FIG. 2. SEM image of HDDR-processed Nd-Fe-B particles (a), microstructure at the particle surface (b) and polished microstructure inside a particle (c). The enlarged surface microstructure is displayed in (d). There do exist Nd-rich GBP inside the particle (white phase at GB in (c)), while lacking Nd-rich GBP on the particle surface (b) and (d).

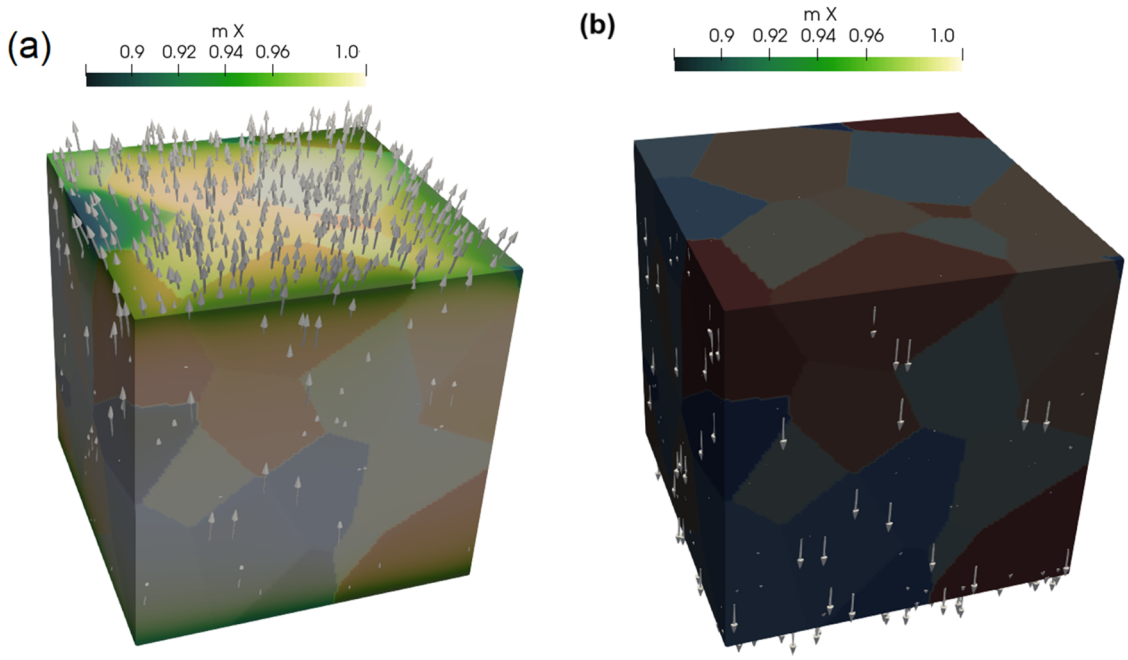

FIG. 3. Spatial resolved magnetization distribution in a cube-shaped Nd-Fe-B magnet without any structural defects under different external field H= −48 kOe (a) and H= −50.4 kOe (b). The arrows show magnetization orientation.

starts on the surface of the magnetic particle due to the strong demagnetization effect on the corners and edges (Fig. 3(a)). This defect-free cube-shaped magnetic particle has a coercivity of 50.4 kOe (Fig. 3(b)). However, if a weak MCA region is present on the particle surface, the coercivity would decrease sharply. For the same-sized cube, with a 3 nm surface layer exhibiting a 50% reduction in MCA, the coercivity decreases from 50.4 kOe to 23 kOe.

As discussed in Sec. III B, almost no Nd-rich GBP is on the surface of the HDDR Nd-Fe-B particles. To gain more insight into the role of Nd-rich GBPs, we perform a micromagnetic simulation to clarify the domain motion between two neighboring grains. Figure 4(a) shows an ideal two-grain model magnet, which has two neighboring 2:14:1 cube-shaped grains without GBP or with a GBP (4nm thickness). The cube grain has an edge length of 128 nm. As shown in Fig. 4(b), the pinning field is 2.5 kOe if no GBP exists between two grains, allowing the domain walls to easily propagate between the grains. The typical Nd-rich GBP ($Nd_{60}Fe_{40}$) has an effective magnetization of 7 kG. An Nd-rich GBP with a thickness of 4 nm markedly enhances the pinning field, increasing it from 2.5 kOe to 22 kOe (Fig. 4(b)). Those results indicate that the lack of Nd-rich GBP on HDDR Nd-Fe-B surface reduces the local coercivity and deteriorates the squareness. As the particle size decreases, the specific surface area increases, further deteriorating squareness and coercivity.

The results also reveal that introducing an Nd-rich GBP around the 2:14:1 grain in the surface defect region can significantly enhance the squareness and coercivity of HDDR-processed Nd-Fe-B powders. Refining the composition or structure of the Nd-rich GBP can further strengthen the domain wall pinning field, thereby improving

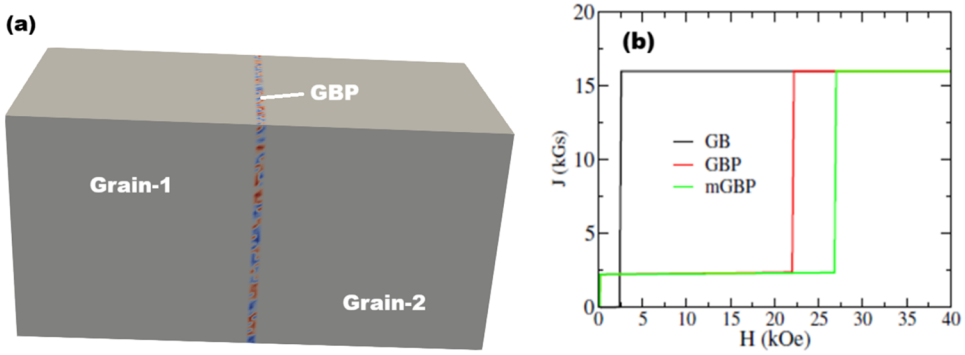

FIG. 4. (a) A model magnet including two grains of 2:14:1; (b) Calculated magnetization curves of model Nd-Fe-B magnets with different grain boundary features. GB—without GBP, GBP—with typical Nd-Fe GBP (Js = 7 kG), mGBP—with modified GBP (Js = 2 kG). In the two-grain microstructure model, each grain has an edge size of 128 nm. The GBP has a thickness of 4 nm.

coercivity and squareness. As shown in Fig. 4, the pinning field can increase from 23 to 27 kOe if the Nd-rich grain is modified by non-magnetic elements such as Cu to reduce its effective magnetization to less than 2.0 kG. Experiments indicate that the grain boundary diffusion process using Pr-Cu or Nd-Cu can substantially increase the coercivity of HDDR Nd-Fe-B powder by up to 40%.[28,29] Those results indicate that surface engineering can improve the coercivity of HDDR Nd-Fe-B.

In summary, the coercivity and squareness of HDDR-processed Nd-Fe-B decrease with decreasing particle size. The microstructure observation reveals the detachment of $Nd_2Fe_{14}B$ grains and the lack of Nd-rich GBP phases from the particle surface. Micromagnetic simulations indicate that demagnetization begins at the particle surface, where these defects are most concentrated, resulting in reduced coercivity and squareness of the demagnetization curves. The reduction in coercivity for smaller HDDR particles is attributed to an increased specific surface area, which reduces nucleation and weakens domain pinning fields during magnetization reversal. By addressing the role of surface defects in coercivity degradation, this study provides insights into improving the coercivity and squareness of both new powder production and recycling strategies, ultimately leading to enhanced performance of bonded magnets. One potential strategy to enhance the performance of HDDR Nd-Fe-B materials involves reducing the fraction of fine particles (<35 μm) and promoting the formation of Nd-rich GBP, which surround the 2:14:1 grains at the particle surfaces. Those GBPs contribute to improved magnetic isolation and enhanced coercivity.

ACKNOWLEDGMENTS

This research was funded by the Critical Materials Innovation Hub funded by the U.S. Department of Energy, Office of Energy Efficiency and Renewable Energy, Advanced Materials and Manufacturing Technologies Office (AMMTO). The work was performed at Ames National Laboratory, operated for the U.S. Department of Energy by Iowa State University of Science and Technology under Contract No. DE-AC02-07CH11358. This manuscript has been authored in part by UT-Battelle, LLC, under contract DE-AC05-00OR22725 with the US Department of Energy (DOE). The US government retains and the publisher, by accepting the article for publication, acknowledges that the US government retains a nonexclusive, paid-up, irrevocable, worldwide license to publish or reproduce the published form of this manuscript, or allow others to do so, for US government purposes. DOE will provide public access to these results of federally sponsored research in accordance with the DOE Public Access Plan (http://energy.gov/downloads/doe-public-access-plan).

AUTHOR DECLARATIONS

Conflict of Interest

The authors have no conflicts to disclose.

Author Contributions

X. B. Liu: Conceptualization (equal); Data curation (equal); Formal analysis (equal); Investigation (equal); Methodology (equal); Visualization (equal); Writing – original draft (equal). **M. S. Kesler**: Conceptualization (equal); Formal analysis (equal); Funding acquisition (equal); Investigation (equal); Project administration (equal); Writing – review & editing (equal). **Z. P. Tener**: Data curation (equal); Investigation (equal); Writing – review & editing (equal). **M. J. Kramer**: Conceptualization (equal); Formal analysis (equal); Methodology (equal); Supervision (equal); Validation (equal); Writing – review & editing (equal). **M. A. McGuire**: Conceptualization (equal); Formal analysis (equal); Methodology (equal); Supervision (equal); Writing – review & editing (equal). **I. C. Nlebedim**: Conceptualization (equal); Formal analysis (equal); Funding acquisition (equal); Methodology (equal); Project administration (equal); Resources (equal); Supervision (equal); Validation (equal); Writing – review & editing (equal).

DATA AVAILABILITY

The data that support the findings of this study are available within the article.

REFERENCES

[1] R. W. McCallum, L. Lewis, R. Skomski, M. J. Kramer, and I. E. Anderson, "Practical aspects of modern and future permanent magnets," Annu. Rev. Mater. Res. **44**, 451–477 (2014).
[2] M. Sagawa, S. Fujimura, H. Yamamoto, Y. Matsuura, and K. Hiraga, "Permanent magnet materials based on the rare earth-iron-boron tetragonal compounds (invited)," IEEE Trans. Magn. **20**(5), 1584–1589 (1984).
[3] J. J. Croat, J. F. Herbst, R. W. Lee, and F. E. Pinkerton, "Pr-Fe and Nd-Fe-based materials: A new class of high-performance permanent magnets (invited)," J. Appl. Phys. **55**(6), 2078–2082 (1984).
[4] T. Takeshita, R. Nakayama, and T. Takeshita, "Nd-Fe-B anisotropic magnet powders produced by the HDDR process," J. Alloys Compd. **193**(1), 259–261 (1993).
[5] T. Takeshita and K. Morimoto, "Anisotropic Nd-Fe-B bonded magnets made from HDDR powders (invited)," J. Appl. Phys. **79**(8), 5040–5044 (1996).
[6] O. Gutfleisch and I. R. Harris, "Fundamental and practical aspects of the hydrogenation, disproportionate, desorption and recombination process," J. Phys. D: Appl. Phys. **29**(9), 2255–2265 (1996).
[7] Y.-F. Yang, X.-H. Wang, N.-T. Quan, Y. Luo, Z.-L. Wang, D.-B. Yu, Z.-K. Wang, T.-H. Li, J.-H. Dong, Y. Lu, and W.-H. Ma, "Enhancing magnetic performance through microstructure optimization in hydrogenation-disproportionation-desorption-recombination Nd-Fe-B powders," J. Magn. Magn Mater. **629**, 173254 (2025).
[8] W. Zhang, Z. Wang, L. Zhang, S. Fan, P. Xia, Y. Shi, R. Wang, and S. Tang, "Preparation and process research of anisotropic Nd-Fe-B spherical magnetic powder," J. Mater. Res. Technol. **39**, 4544–4552 (2025).
[9] G. Bacchetta, F. Orlandini-Keller, C. Flament, L. Magnier, S. Luca, C. Rado, and J. P. Garandet, "High-temperature hydrogen-induced phase transformation in Nd-Fe-B alloys," J. Alloys Compd. **1010**, 177980 (2025).
[10] J. An, J. Wen, X. Liu, X. Li, and J. Hu, "Influence of preparation processes with or without long-time homogenization heat treatment on performance of Nd–Fe–B HDDR products," J. Magn. Magn Mater. **598**, 172076 (2024).
[11] R. S. Sheridan, I. R. Harris, and A. Walton, "The development of microstructure during hydrogenation-disproportionation-desorption-recombination treatment of sintered neodymium-iron-boron-type magnets," J. Magn. Magn Mater. **401**, 455–462 (2016).
[12] H. Zhao, W. Yin, G. Ding, J. Ju, X. Tang, R. Chen, J. Yuan, and A. Yan, "Preparation of anisotropic (Ce, Nd, Pr)-Fe-B powder with HDDR method from wasted sintered magnets," J. Magn. Magn Mater. **562**, 169745 (2022).
[13] I. Poenaru, E. A. Patroi, D. Patroi, A. Iorga, and E. Manta, "HDDR as advanced processing method and recycling technology to address the rare-earth resource

criticality in high performance $Nd_2Fe_{14}B$ magnets production," J. Magn. Magn Mater. **577**, 170777 (2023).
[14]T. Tomida, P. Choi, Y. Maehara, M. Uehara, H. Tomizawa, and S. Hirosawa, "Origin of magnetic anisotropy formation in the HDDR-process of $Nd_2Fe_{14}B$-based alloys," J. Alloys Compd. **242**(1–2), 129–135 (1996).
[15]J. Han, A. Sun, Y. Xiao, X. Liu, and R. Wang, "Anisotropic characteristic in HDDR $Nd_{13}Fe_{80}B_7$," J. Univ. Sci. Technol. Beijing **10**(3), 26–29 (2003).
[16]S. Liu, J. Han, H. Du, C. Wang, H. chen, and Y. Yang, "Microstructural evolutions of $Pr_{13}Fe_{80}B_7$ alloys during solid HDDR process," J. Magn. Magn Mater. **312**(2), 337–341 (2007).
[17]X. B. Liu, M. S. Kesler, M. F. Besser, M. J. Kramer, M. A. McGuire, and I. C. Nlebedim, "Effect of processing hydrogen pressure on magnetic properties of HDDR Nd-Fe-B magnet," IEEE Trans. Magn. **57**(2), 12100604 (2021).
[18]R. Ramesh, G. Thomas, and B. M. Ma, "Magnetization reversal in nucleation controlled magnets. II. Effect of grain size and size distribution on intrinsic coercivity of Fe-Nd-B magnets," J. Appl. Phys. **64**(11), 6416–6423 (1988).
[19]T. T. Sasaki, T. Ohkubo, Y. Takada, T. Sato, A. Kato, Y. Kaneko, and K. Hono, "Formation of non-ferromagnetic grain boundary phase in a Ga-doped Nd-rich Nd–Fe–B sintered magnet," Scr. Mater. **113**, 218–221 (2016).
[20]D. J. Branagan, M. J. Kramer, Y. L. Tang, and R. W. McCallum, "Maximizing loop squareness by minimizing gradients in the microstructure," J. Appl. Phys. **85**(8), 5923–5925 (1999).
[21]W. F. Brown, Jr., *Micromagnetics* (Wiley, New York, 1963).
[22]H. Kronmüller, R. Fischer, M. Seeger, and A. Zern, "Micromagnetism and microstructure of hard magnetic materials," J. Phys. D: Appl. Phys. **29**(9), 2274–2283 (1996).
[23]J. Fidler and T. Schrefl, "Micromagnetic modelling - The current state of the art," J. Phys. D: Appl. Phys. **33**(15), R135–R156 (2000).
[24]A. Vansteenkiste, J. Leliaert, M. Dvornik, M. Helsen, F. Garcia-Sanchez, and B. van Waeyenberge, "The design and verification of MuMax3," AIP Adv. **4**(10), 107133 (2014).
[25]A. Vansteenkiste, B. V De Wiele, and B. V. de Wiele, "MuMax: A new high-performance micromagnetic simulation tool," J. Magn. Magn Mater. **323**(21), 2585–2591 (2011).
[26]X. B. Liu and I. C. Nlebedim, "Segregation of Al and its effect on coercivity in Nd-Fe-B," AIP Adv. **14**(1), 015030 (2024).
[27]J. Coey, *Magnetism and Magnetic Materials* (Cambridge University Press, 2010).
[28]T. Ueno, K. Saito, M. Yano, M. Harada, T. Shoji, N. Sakuma, A. Manabe, A. Kato, U. Keiderling, and K. Ono, "Magnetization reversal process in Pr-Cu infiltrated Nd-Fe-B nanocrystalline magnet investigated by small-angle neutron scattering," IEEE Trans. Magn. **50**(11), 2103104 (2014).
[29]Z. Lin, J. Han, M. Xing, S. Liu, R. Wu, C. Wang, Y. Zhang, Y. Yang, and J. Yang, "Improvement of coercivity and thermal stability of anisotropic $Nd_{13}Fe_{79.4}B_7Nb_{0.3}Ga_{0.3}$ powders by diffusion of Pr-Cu alloys," Appl. Phys. Lett. **100**(5), 052409 (2012).